Low-Profile Array With Reduced Radar Cross Section by Using Hybrid Frequency Selective Surfaces

Simone Genovesi, *Member, IEEE*, Filippo Costa, *Member, IEEE*, and Agostino Monorchio, *Fellow, IEEE*

***Abstract*—A solution for reducing the radar cross section (RCS) of a microstrip antenna based on the use of frequency selective surfaces (FSSs) is described. The goal is accomplished by replacing the solid ground plane of the device with a hybrid structure comprising a suitable FSS. The behavior of the hybrid ground plane illuminated by a plane wave is analyzed by using a periodic method of moments (PMM), and it is modeled by resorting to a transmission-line equivalent circuit. Similarly, the propagation of the quasi-TEM mode along the modified feeding line of the array is represented by an equivalent circuit for surface waves. The two simplified analyses provide useful design criteria for the hybrid ground structure. The presented solution guarantees a decrease of the out-of-band radar signature of the target while preserving the desired in-band radiation characteristics of the low-profile array. A careful comparison to alternative configurations employing different ground planes has revealed the superior performance of the proposed design. Measurements on a realized prototype show a good agreement with simulations and prove the reliability of the design approach.**

***Index Terms*—Frequency selective surfaces (FSSs), radar cross section reduction (RCSR).**

I. Introduction

ANTENNAS significantly contribute to the overall radar cross section (RCS) signature of target objects such as naval ships and airborne vehicles. The study of methods that allow reducing the RCS of an antenna is therefore of great practical interest. Many solutions have been proposed to obtain a radar cross section reduction (RCSR). Among them, the shaping of the target surfaces and the use of radar absorbing materials (RAMs) are certainly among the most practiced designs even if they use a different mechanism to decrease the RCS. In fact, the former approach modifies the target shape or orientation to deflect the scattered energy away from the detecting radar [1], [2], whereas RAMs basically convert the radio frequency energy into heat [3]–[5]. Other solutions involve the use of tapered resistive sheets in the antenna [6] or in the radome [7] and passive or active cancellation technology [8]. However, since the RCSR always implies a tradeoff among the decrease of radar signature, the increase in cost or maintenance of the system, and the global performance, an accurate design has to balance advantages against disadvantages.

Manuscript received December 18, 2010; revised September 24, 2011; accepted November 26, 2011. Date of publication March 01, 2012; date of current version May 01, 2012.

The authors are with the Dipartimento di Ingegneria dell'Informazione, University of Pisa, 56122 Pisa, Italy (e-mail: simone.genovesi@iet.unipi.it; filippo.costa@iet.unipi.it; a.monorchio@ieee.org).

Color versions of one or more of the figures in this paper are available online at http://ieeexplore.ieee.org.

Digital Object Identifier 10.1109/TAP.2012.2189701

As in the case of a single antenna, the RCS of an array is determined by an antenna component and by a structural term [8]–[11]

$$\sigma = |\sqrt{\sigma_{\rm s}} - (1-\Gamma_{\rm a})\sqrt{\sigma_{\rm a}}e^{j\phi}|^2 \tag{1}$$

where σ is the total RCS of the target, $\sigma_{\rm s}$ is related to the field scattered by the short-circuited antenna, $\sigma_{\rm a}$ represents the field scattered by the antenna that involves the value of the port impedance, $\Gamma_{\rm a}$ is the antenna reflection coefficient, and ϕ is the relative phase between the two terms.

Our investigation will focus on the reduction of the structural term $\sigma_{\rm s}$ of an antenna array, and it will be analyzed under the short-circuit condition of the feeding port. The idea of replacing the ground plane of an antenna with a frequency selective surface (FSS) to reduce the radar cross section dates back to 2003 when this concept was applied to a reflectarray [12]. The reflectarray is a passive radiator, and the application of this principle is straightforward since the FSS has to behave as a solid electric conductor for plane waves. Conversely, the application of the same concept to reduce the RCS of a printed microstrip array antenna is more challenging since the modified ground plane has also to support the quasi-TEM mode. Indeed, while the reflectarray is illuminated by a plane wavefront with the electric field parallel (or almost parallel) to the printed pattern, a microstrip antenna is characterized by electric fields orthogonal to the ground plane both below the radiating patches and across the feeding network.

In the recent literature [13], the use of a bandstop FSS has been exploited to reduce the RCS of array of monopoles orthogonally placed on a perfect electric conductor (PEC). However, the final design of the radiating structure is cumbersome and not mechanically robust; additionally, the main RCS reduction is obtained along a direction where the array is not able to scan.

The aim of the present work is to describe a strategy to decrease the structural RCS of a common patch array antenna at the out-of-band frequencies by replacing the ground plane with a suitable hybrid structure. This paper is organized as follows. The design of the FSS unit cell is addressed in Section II, and an equivalent circuit model that predicts the frequency response of the infinite screen illuminated by a plane wave is described. In Section III, the ability of the modified ground plane to support the quasi-TEM mode is investigated through a transmission-line model. The extracted lumped element circuit parameters are then discussed. Section IV is devoted to assess the performance of the microstrip antenna backed by the aforementioned hybrid ground plane in terms of radiation characteristics and the achieved RCSR.

0018-926X/$31.00 © 2012 IEEE

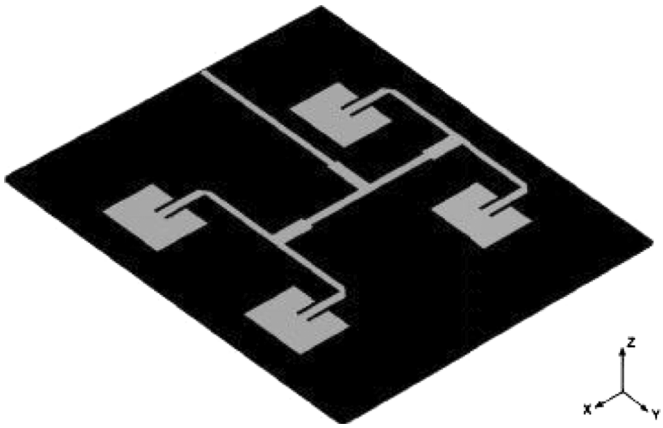

Fig. 1. Original array configuration with solid ground plane that represents the reference case.

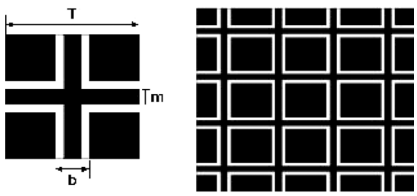

Fig. 2. (a) Unit cell of the passband FSS screen, (b) overall FSS screen. The black color indicates the conductive surface.

II. Frequency Selective Surface Design

As a test case, a microstrip patch array antenna working at 2.5 GHz is considered. The antenna is printed on a grounded FR4 dielectric substrate ($\varepsilon_r = 4.4$, tg loss $= 0.02$, thickness $h = 2.0$ mm) for limiting the cost of the prototypes. The reference antenna with metallic ground is shown in Fig. 1.

The total-reflection band of the FSS has to match the antenna resonance frequency in order to allow the proper radiation of the device. Outside the stopband, as soon as the FSS becomes transparent, the overall structural RCS of the array will be reduced in correspondence of its passband.

It is desirable that the FSS ground exhibits a frequency response as stable as possible with respect to the incidence angle in order to have a satisfying level of RCSR not only for monostatic probing, but also for bistatic interrogation.

Let us suppose to require as a goal an RCSR in a given frequency bandwidth that is 6.0–8.0 GHz. A design that satisfies these specifications is presented in Fig. 2. The unit cell printed on the lower part of the FR4 substrate is in Fig. 2(a), where $T = 8.0$ mm, $m = 1.0$ mm, and $b = 2.0$ mm, and the overall screen is reported as well in Fig. 2(b).

The analysis of the FSS has been performed by using a periodic method of moments (PMM) [14]. As it is apparent from Figs. 3 and 4, the frequency response is reasonably stable for both TE and TM polarization also for off-normal incidence angles θ. More in detail, the reflection coefficient of the infinite FSS is around -5.0 dB or lower between 6.0–8.0 GHz for both polarizations and up to 45°, although it suffers from a small and predictable narrowing of the TE passband bandwidth. On the other hand, the FSS exhibits a PEC-like response for both polarizations around 2.5 GHz. Let us observe the reflection behavior for TM oblique incident waves. It provides a useful insight for evaluating the performance of the FSS when employed as ground plane of a microstrip array. As a matter of fact, electric fields below the patches of the printed antenna are mainly orthogonal to the ground plane as it happens in the case of grazing TM incident plane waves. It is evident from the inset of Fig. 4 that the reflectivity of the surface diminishes as the incident angles approach 90°. The limited reflectivity of the periodic FSS ground for grazing TM waves may render such structure unsuitable for operating as a ground plane for a microstrip antenna. This aspect will be thoroughly addressed in Section III, where an alternative configuration of the ground plane will be proposed.

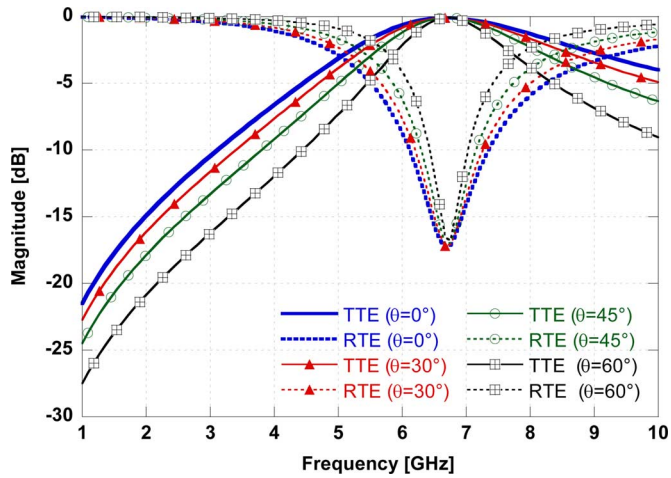

Fig. 3. Frequency response of the FSS screen for TE polarization at various incidence angles: reflection (RTE) and transmission (TTE) coefficient.

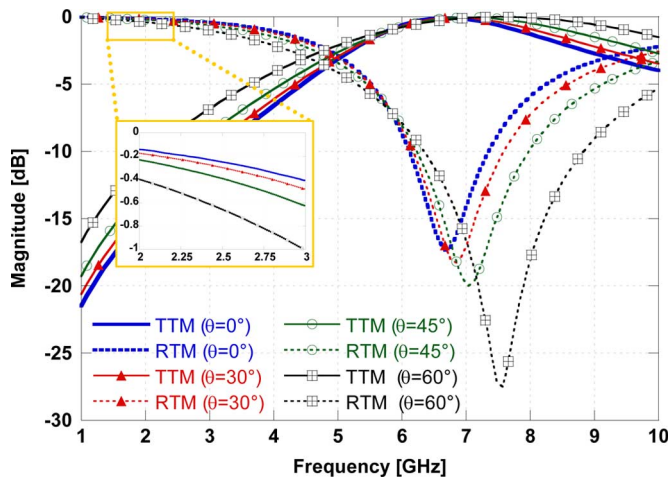

Fig. 4. Frequency response of the FSS screen for TM polarization at various incidence angles: reflection (RTM) and transmission (TTM) coefficient.

An equivalent transmission-line network can be adopted to describe the frequency response of the periodic surface [15]–[17] for a normal or oblique incident plane wave. A parallel L_0C_0 circuit is employed to take into account the FSS, whereas transmission-line sections represent the involved dielectric substrates as reported in Fig. 5(a). Depending on the considered polarization, each section of the transmission line has its own propagation constant and characteristic impedance

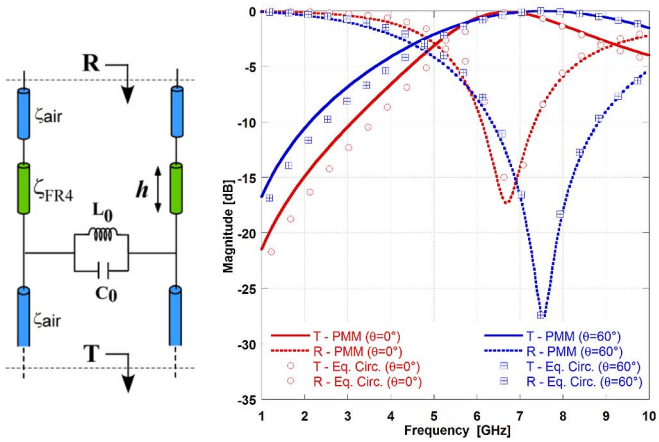

(a) (b)

Fig. 5. Equivalent circuit model: (a) transmission line with reflection (R) and transmission (T) coefficient fitting the frequency behavior of the FSS screen; (b) comparison between simulation with PMM and equivalent model for a TM plane wave for $\theta = 0$ and 60°.

TABLE I
CIRCUIT PARAMETERS VALUES FOR THE INFINITE FSS (TM POLARIZATION)

	θ= 0°	θ= 60°
L_0	1.94 nH	1.70 nH
C_0	0.217 pF	0.26 pF

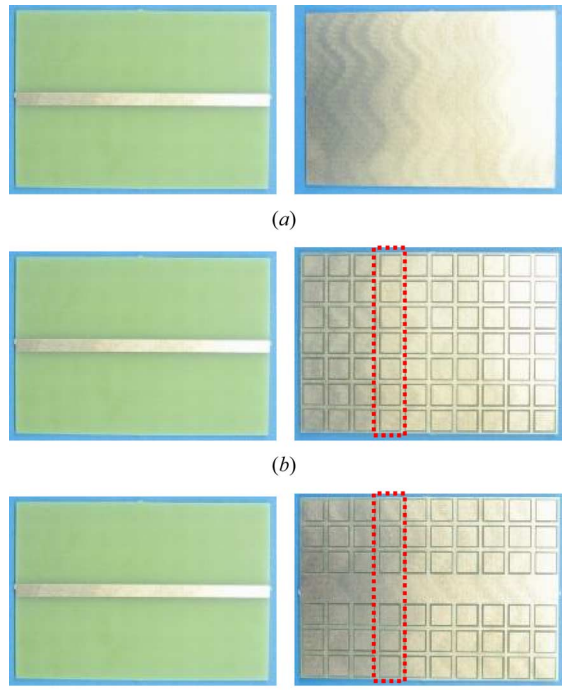

(a) (b) (c)

Fig. 6. Prototypes of the three investigated ground planes of the feeding lines: (a) solid ground, (b) FSS ground, and (c) hybrid ground. The unit section modeled in the equivalent circuit is highlighted by the dotted rectangle.

that depends on the plane wave incidence angle θ and dielectric permittivity of the medium ε_r. For a TE/TM plane wave and an FR4 dielectric substrate, we obtain

$$k_z = \sqrt{\varepsilon_r k_0^2 - k_t^2} \quad \zeta^{TM} = \frac{k_z}{\omega \varepsilon_r \varepsilon_0} \quad \zeta^{TE} = \frac{\omega \mu_r \mu_0}{k_z} \qquad (2)$$

where k_0 is the free-space propagation constant, k_t is the transverse wave vector ($k_t = k_0 \sin(\theta)$), and θ is the incident angle. The value of L_0 and C_0 are determined by matching the full-wave data with the frequency response of the equivalent transmission line for each required value of θ. The comparison between the reflection and transmission coefficient of the full wave simulation and of the equivalent circuit is reported in Fig. 5(b) for the case of a TM plane wave. The circuit parameter values of the FSS are reported in Table I. A similar result can be achieved for a TE plane wave. It is interesting to notice that for the TM polarization, as the angle θ increases, the value of L_0 decreases while the value of C_0 rises.

III. ANALYSIS OF THE QUASI-TEM PROPAGATION ALONG MODIFIED GROUNDS

The simplest solution for designing a low-RCS microstrip array is to replace the metallic ground with a periodic frequency selective surface. However, since the microstrip line and the patch antenna have to support the quasi-TEM mode [18], a careful study to verify the effect of the patterned ground plane on the feeding network performance is required. Additionally, the portion of the ground plane below the radiating patches must be totally reflecting for the orthogonal electric fields supported by the microstrip antenna (i.e., TM grazing waves) in order to limit as much as possible undesired back radiation and the consequent unwanted energy loss. In order to focus on this aspect, we have tested the transmission properties of the three different transmission lines shown in Fig. 6.

A microstrip line with characteristic impedance equal to 50 Ω has been printed on the top of an FR4 dielectric slab. On the opposite side of the FR4 slab, three different grounds have been printed: (a) a solid ground plane, (b) an FSS ground, and (c) a hybrid ground comprising a PEC area beneath the microstrip line surrounded by FSS unit cells. All of the three samples have equal size of 8.0×5.6 cm^2, which corresponds to 10×7 FSS unit cells. The simulated and measured transmission coefficients of the analyzed transmission lines are shown in Fig. 7.

It can be noticed that the level of transmission is slightly different between simulated and measured results, and this is due to the uncertainty on the dielectric permittivity of the substrate. However, the relative difference among the three configurations is preserved. In fact, it is interesting to observe that both the simulated and the measured transmission level of the finite FSS ground [Fig. 6(b)] is around 0.5 dB lower than the solid ground plane within the operating band of the antenna. Conversely, the hybrid configuration [Fig. 6(c)] has almost the same transmission level of the PEC ground within the array bandwidth, thus proving that this modified ground plane does not significantly affect the power propagation of the signal along the feeding lines.

A first-order analysis of a transmission line with a modified ground plane is carried out by resorting to a lumped-element model [19]–[21]. The model is useful to get some insight into the propagation mechanism that determines the different transmission losses observed in the FSS and hybrid ground plane.

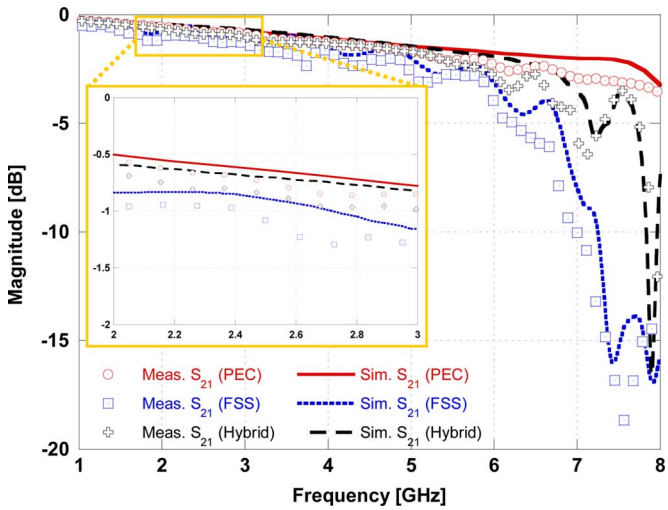

Fig. 7. Comparison between the simulated and measured transmission level of the three ground planes.

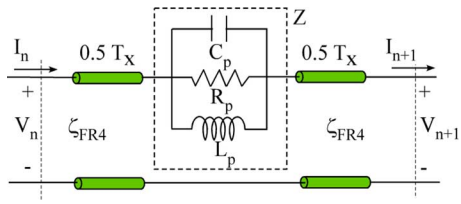

Fig. 8. Equivalent circuit for the section.

It is worthwhile underlining that in Section II we adopted an equivalent circuit to describe the ability of the modified ground plane to be reflective or transparent to a normal or oblique incident plane wave. Conversely, in this case we are investigating the capacity of the modified ground plane to support the quasi-TEM mode and to prevent undesired energy loss or radiation. First of all, we define the unit section (Fig. 6) to be modeled by using the equivalent circuit illustrated in Fig. 8. The capacitor and the inductor represent the FSS selectivity, while the resistor R_p takes into account radiation losses.

The values of the resistor and lumped elements of the proposed equivalent circuit can be extracted by using a full-wave analysis to characterize the unit section with the correspondent $ABCD$ matrix

$$\begin{bmatrix} A & B \\ C & D \end{bmatrix} = \begin{bmatrix} \cos\theta & i\zeta_{\mathrm{FR4}}\sin\theta \\ \frac{i\sin\theta}{\zeta_{\mathrm{FR4}}} & \cos\theta \end{bmatrix} \begin{bmatrix} 1 & Z \\ 0 & 1 \end{bmatrix} \begin{bmatrix} \cos\theta & i\zeta_{\mathrm{FR4}}\sin\theta \\ \frac{i\sin\theta}{\zeta_{\mathrm{FR4}}} & \cos\theta \end{bmatrix} \tag{3}$$

where $\theta = kT_x/2$, k is the free-space propagation constant and ζ_{FR4} is the characteristic impedance of the line. Once we have described the equivalent circuit of the unit section, we employ the well-known analysis for a periodically loaded transmission line [18] to calculate the frequency response of the overall structure. More in detail, in our case the final matrix describing the 10 unit sections of the transmission lines reported in Fig. 6 is equal to

$$\begin{bmatrix} A & B \\ C & D \end{bmatrix}_{\mathrm{Total}} = \left(\begin{bmatrix} A & B \\ C & D \end{bmatrix} \right)^{10}. \tag{4}$$

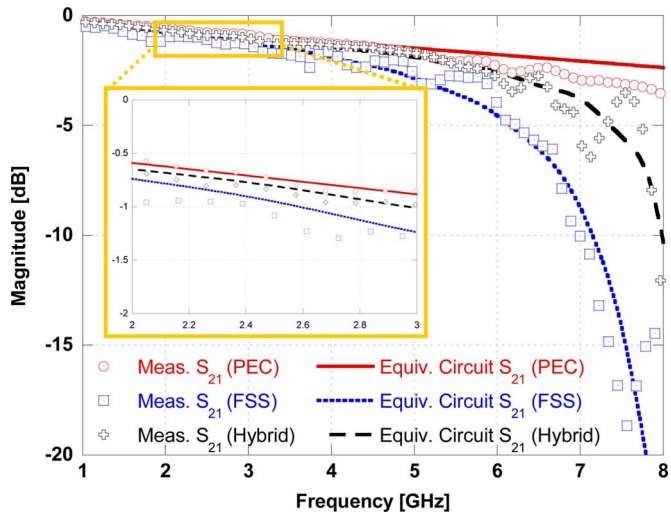

Fig. 9. Comparison between levels of transmission obtained from measurements and the equivalent circuit.

TABLE II
CIRCUIT PARAMETERS VALUES FOR THE TWO MODIFIED GROUND PLANES

	FSS	Hybrid
L_p	0.420 nH	0.371 nH
C_p	0.545 pF	0.515 pF
R_p	140 Ω	345 Ω

The computed lumped parameters of the unit section are reported in Table II.

The comparison between the measurements and the analytic model is reported in Fig. 9 for the grounds illustrated in Fig. 6.

It is interesting to compare the values of the parameters reported in Table II to those obtained from the model for plane wave incidence illustrated in Table I. Indeed, the inductance L_p decreases with respect to L_0 for both the FSS and hybrid configuration, while the capacitance C_p increases with respect to the C_0. As we already pointed out in Section II, L_0 and C_0 for TM polarization are decreasing and increasing, respectively, as the angle θ is more and more off the normal direction. Therefore, the equivalent values we have found in this section confirm the previously observed trend. Considerations on the radiation losses of the different structures can be derived from the values of the resistance R_p. In particular, the R_p value for the FSS ground is lower than the corresponding resistance of the hybrid screen. It is useful to keep in mind that radiation loss increases as the value of the parallel resistor decreases [19]. Finally, in order to analyze the dispersive properties of the surfaces, the phase of the transmission coefficient between the two-port microstrip devices is reported in Fig. 10. The phase of the transmitted signal reveals that only the FSS ground is slightly dispersive around the array working frequency, namely 2.5 GHz. The hybrid ground does not introduce any distortion in the transmitted signal. In conclusion, the hybrid surface results in the most promising solution for designing a low-RCS ground plane for a microstrip antenna.

IV. PERFORMANCE OF THE REDUCED RCS ANTENNA

In the two previous sections, two separate studies have been carried out in order to evaluate the response of a modified ground plane when it is illuminated by a plane wave or when it

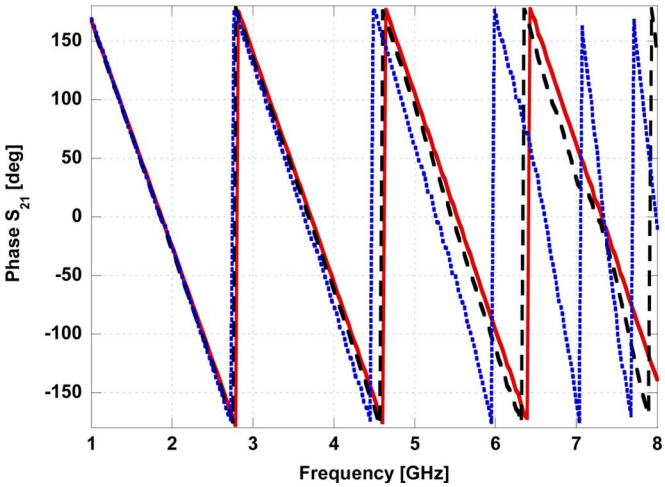

Fig. 10. Phase of the transmitted signal in the case of the solid PEC ground plane (continuous line), the hybrid ground (dashed line), and a finite FSS ground plane (dotted line).

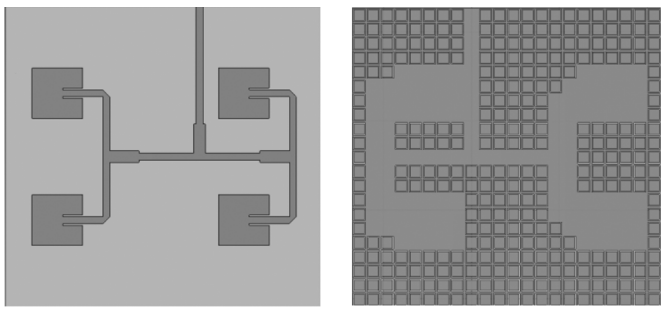

Fig. 11. (a) Top and (b) bottom view of the antenna with hybrid ground plane.

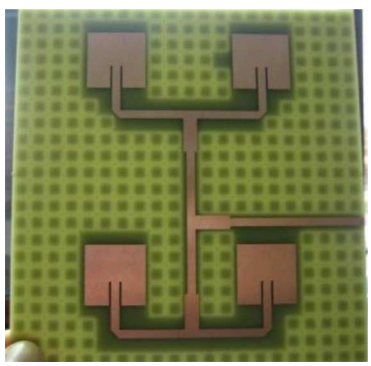

Fig. 12. Front view of the modified patch antenna microstrip array.

supports the propagation of the quasi-TEM mode. The analysis allowed us to identify a promising hybrid structure. In this section, we verify if it guarantees an efficient radiation and a significant reduction of the RCS at the same time.

The original array has been therefore modified into the structure shown in Fig. 11.

The prototype of the proposed array with the hybrid ground plane is shown in Fig. 12. The size is 17.6×16.8 cm^2, which corresponds to 22×21 unit cells. As it is apparent, the solid ground plane of the original configuration has not been completely removed. In fact, as discussed in Section III, these portions of the metallic ground underneath the microstrip lines and

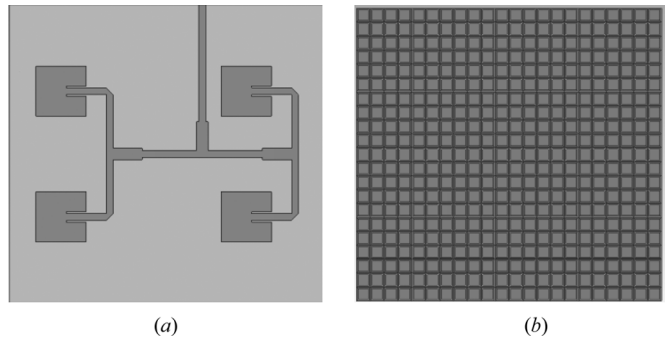

Fig. 13. (a) Top and (b) bottom view of the antenna with the finite FSS screen as a ground plane.

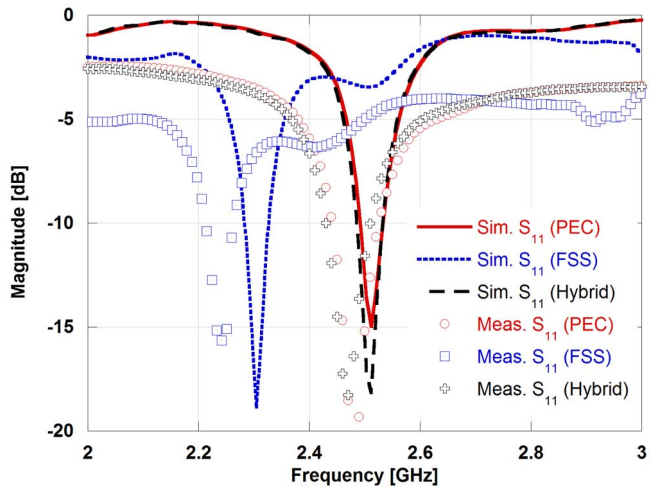

Fig. 14. Comparison among the magnitude of the S_{11} parameter of the array with solid ground plane, finite FSS ground plane, and hybrid one.

the patches allow the antenna to radiate efficiently. Although the radiating patch elements and the feed line printed on the top of the dielectric slab determine a contribution to the RCS that cannot be removed, it has to be pointed out that such configuration provides a reduction of the structural RCS. All the simulations have been performed by using CST Microwave Studio 2010 [22].

A. Radiation Performance

A potential drawback in replacing the solid ground plane can be a degradation of the array bandwidth with a consequent necessity of additional tuning of the radiating element. To this aim, we consider both the hybrid ground plane (Fig. 11) and the finite FSS screen (Fig. 13), and we compare the magnitude of the S_{11} of the antenna with these modified ground planes against the S_{11} of the original antenna.

As it is apparent from Fig. 14, the solution exploiting the hybrid ground plane does not perturb the original S_{11}, whereas the one with the finite FSS ground encounters a larger frequency shift. The small shift between measured and simulated results is imputable to the uncertainty of the FR4 substrate characteristics.

The other crucial issue is the preservation of the original antenna radiation pattern as well as the peak gain. In order to perform a comprehensive study of the structure, an additional case leading to a RCS reduction has been considered.

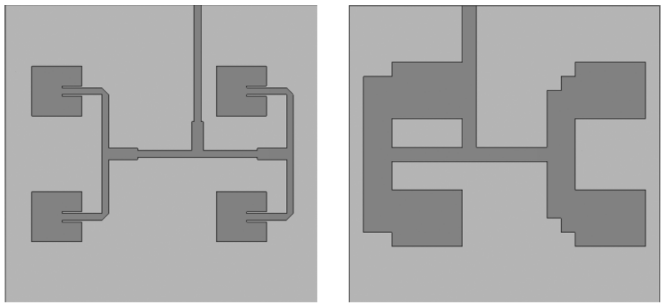

(*a*) (*b*)

Fig. 15. (a) Top view and (b) bottom view of the array with minimum ground plane where all the FSS unit cells are removed.

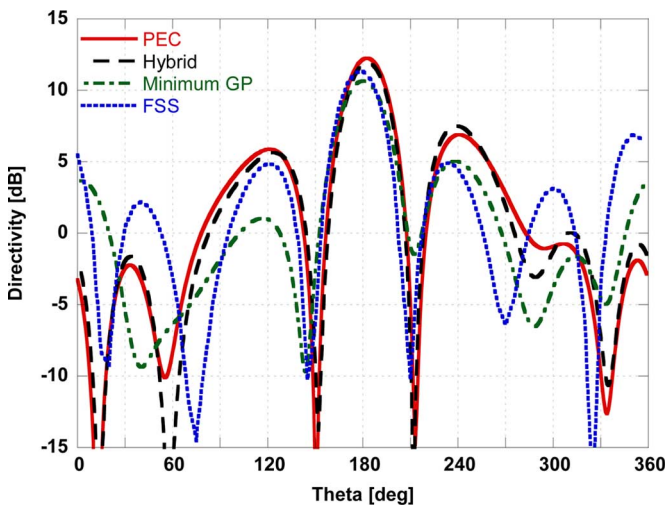

Fig. 16. Comparison among the gain at 2.5 GHz in the $\phi = 0°$ for the different ground planes.

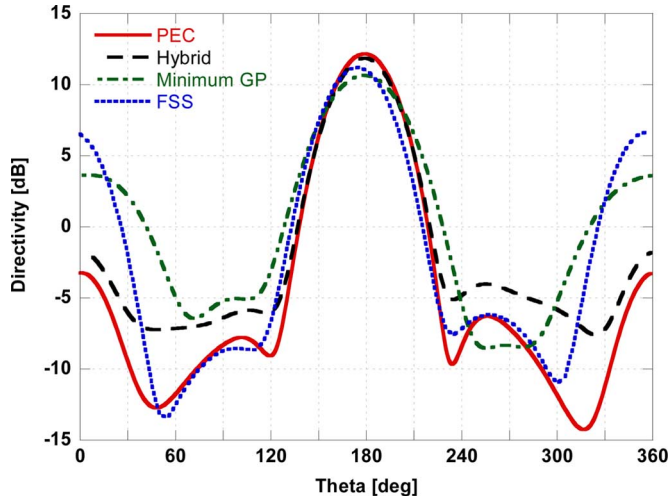

Fig. 17. Comparison among the gain at 2.5 GHz in the $\phi = 90°$ for the different ground planes.

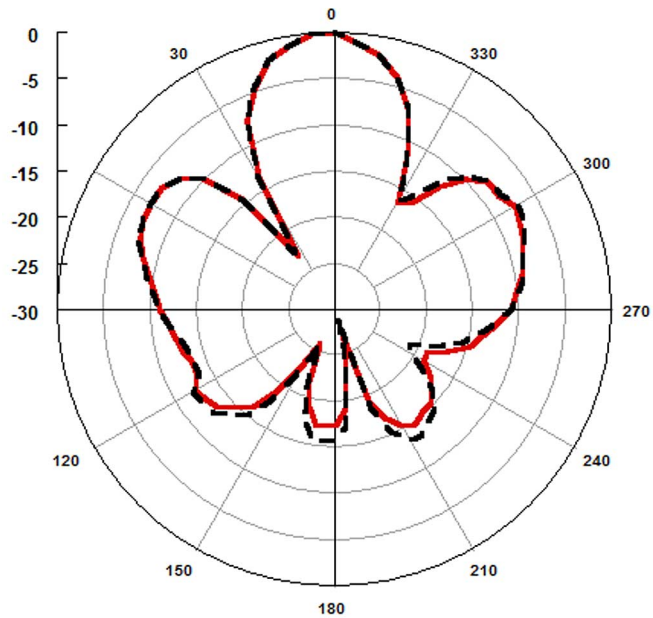

Fig. 18. Comparison between the measured radiation patterns on the E-plane of the array with solid ground plane (solid line) and the array with hybrid ground plane (dashed line).

This additional configuration named "minimum ground plane (GP)" and reported in Fig. 15 comprises a reduced metallic ground plane with all the additional FSS unit cells removed. This case is analyzed to undoubtedly prove the importance of the FSS cells.

A comparison among the radiation patterns of the four analyzed configurations is illustrated in Figs. 16 and 17 for the E- and H-plane, respectively.

The antenna array with the hybrid ground plane provides a boresight directivity close to the one offered by the antenna with solid ground (0.3 dB loss, from 12.0 to 11.7 dB) and a comparable front-to-back ratio (from 15.0 to 13.7 dB). The configuration with the minimum GP ground exhibits a lower broadside directivity (10.6 dB) and a worse front-to-back ratio (7.0 dB), while the antenna with FSS ground has an acceptable directivity equal to 11.2 dB, but a back radiation of 6.5 dB, which determines the worst front-to-back ratio (4.7 dB). The analysis of the radiation patterns of the three low-RCS configurations demonstrates that only the hybrid ground plane configuration has a negligible impact on the radiation performance. It is interesting to observe how the same conclusion could be drawn also examining the values of R_p reported in Table II. Indeed, the highest value of R_p in the case of the hybrid ground plane expresses the lower radiation loss suffered by the signal below the resonance of the parallel L_pC_p circuit.

A final verification is accomplished by comparing the measured radiation patterns of the antenna with the solid ground plane and with the modified ground. The radiation patterns reported in Figs. 18 and 19 agree very well with each other, proving that the presence of the modified ground has a very small effect on the pattern shape.

B. Radar Cross Section Reduction

In this section, the scattering properties of the proposed antenna are compared to those of the reference structure with metallic ground plane. The results are obtained both by the full-wave simulator and through reflection measurements on the manufactured prototypes.

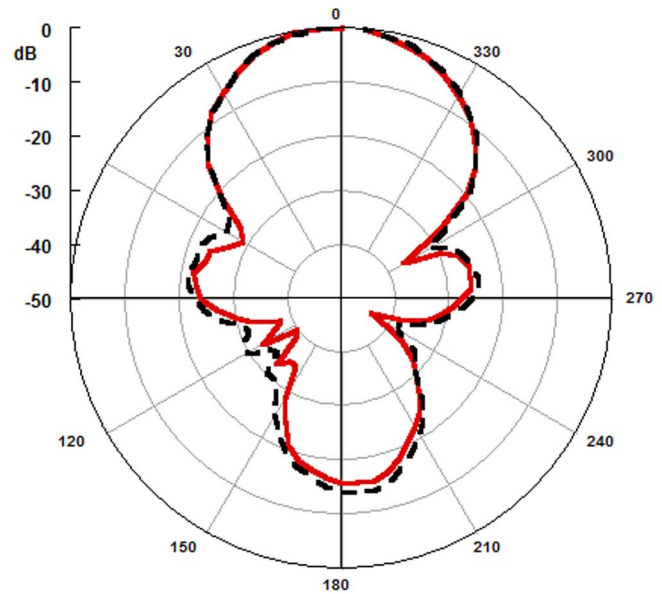

Fig. 19. Comparison between the measured radiation patterns on the H-plane of the array with solid ground plane (solid line) and the array with hybrid ground plane (dashed line).

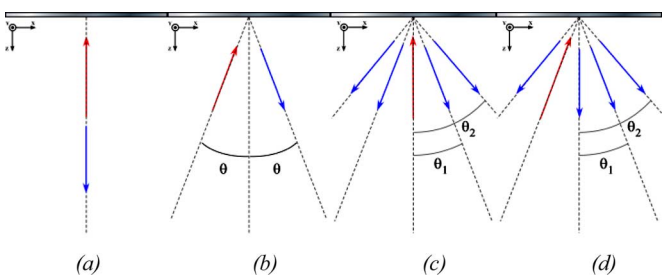

Fig. 20. Analysis for different configurations of the impinging (upward-pointing arrow) and the scattered fields (downward-pointing arrows). (a) Monostatic for normal incidence within $[f_1, f_2]$. (b) Bistatic for oblique incidence within $[f_1, f_2]$. (c) Bistatic for normal incidence at f_0. (d) Bistatic for oblique incidence at f_0.

The simulated RCS exhibited by the antenna array with the hybrid FSS ground plane is compared against the one of the microstrip antenna with solid metallic ground plane both for monostatic and bistatic configurations. More in detail, we have considered the variation of the RCS as a function of frequency within the bandwidth [$f_1 = 1$ GHz–$f_2 = 10$ GHz] for the two configurations reported in Fig. 20(a) and (b). The results are illustrated in Figs. 21 and 22 for TE and TM polarization, respectively.

As it is apparent, the antenna with the hybrid ground plane is characterized by a strong RCS reduction within the transmission band of the FSS since the incoming signals passes unaltered through the multilayer. The RCS reduction in the same frequency band is preserved also for oblique incident angles since the frequency response of the FSS is characterized by a high angular stability. We have also analyzed the variation of the RCS as a function of angle θ in $(-90°, 90°)$ at the fixed frequency $f_0 = 7$ GHz for the cases shown in Fig. 20(c) and (d). The results are illustrated in Fig. 23 for a normal impinging

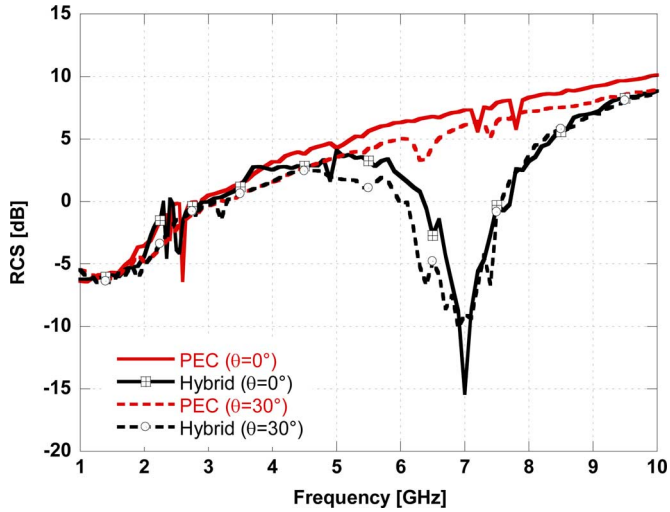

Fig. 21. Comparison between the RCS of the two structures for a normal and oblique incident TE plane wave (E incident field along x-axis).

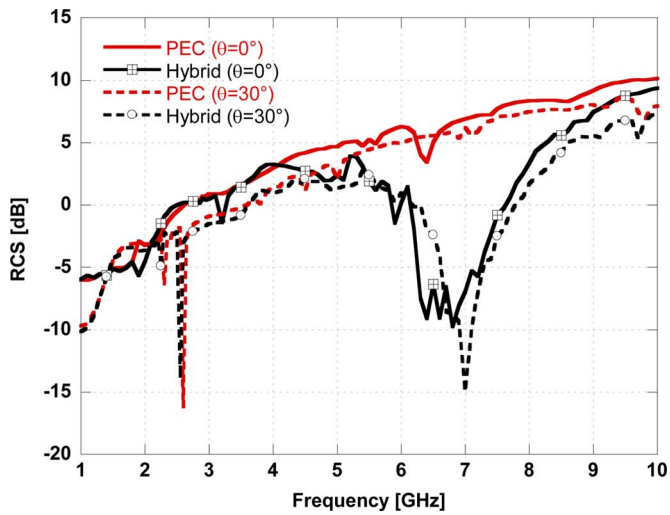

Fig. 22. Comparison between the RCS of the two structures for a normal and oblique incident TM plane wave (E incident field along y-axis).

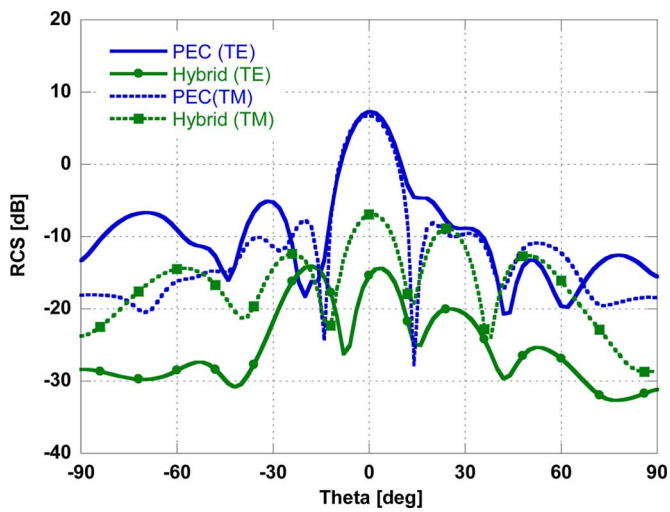

Fig. 23. Comparison between the RCS of the two structures for a normal incident TE and TM plane wave at $f_0 = 7$ GHz.

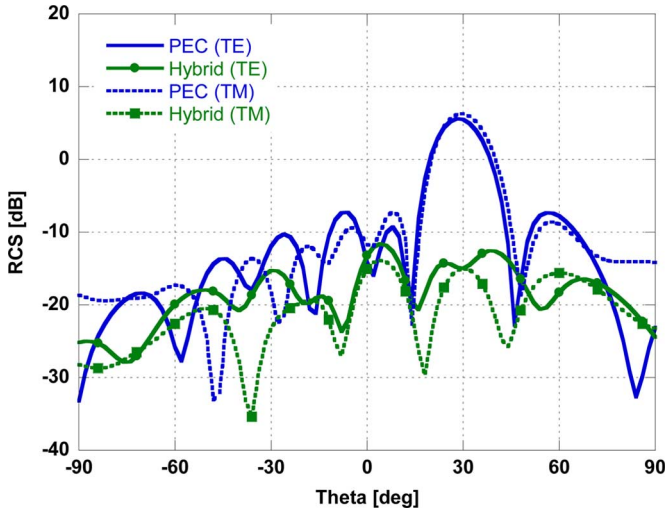

Fig. 24. Comparison between the RCS of the two structures for an oblique ($\theta = 30°$) incident TE and TM plane wave at $f_0 = 7$ GHz.

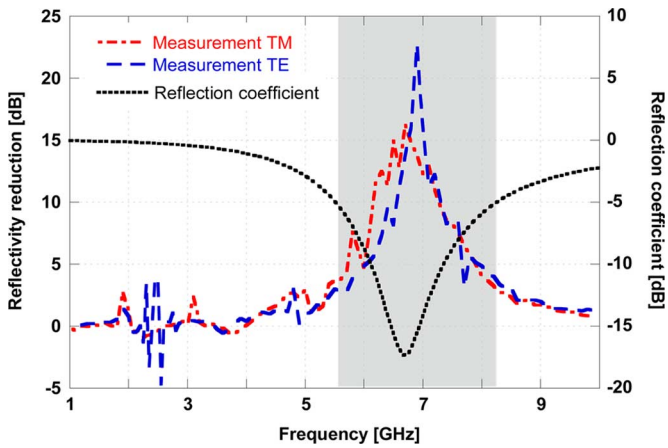

Fig. 25. Comparison between the reflection coefficient of the infinite FSS and the measured reflectivity reduction for TE and TM incidence.

plane wave, and in Fig. 24 for a probing radiation from $\theta = 30°$ for both polarizations.

As it is apparent from Figs. 23 and 24, the decreasing of the RCS can be appreciated not only for a normal impinging plane wave, but also for a off-normal direction of arrival of the probing radiation. This proves that a good RCS reduction is achieved by the hybrid ground plane in all directions within the individuated frequency band and also for oblique incidence. It is worthwhile to notice that the asymmetry of the scattered radiation is due to the presence of the feeding network that breaks the symmetry of the antenna array.

The reduction of the reflectivity is confirmed by measurements on the manufactured prototype reported in Fig. 12. In the measurement setup, the device under test is illuminated by using a wideband horn antenna, and the scattered signal is recovered by an identical wideband horn antenna. The scattering parameters of the antenna have been measured by using an Agilent E5071C vector network analyzer. The distance between the horn antennas and the microstrip array was 1 m.

Fig. 25 reports the reflectivity reduction of the modified antenna with respect to the reference one with the metallic ground at normal incidence for both polarizations. The result is compared to the reflection coefficient of the infinite FSS.

It is possible to observe that the most relevant RCS reduction for both TE and TM polarization occurs in correspondence of the frequency band where the infinite FSS presents a reflection coefficient lower than -5.0 dB. This simple design criterion has a great practical usefulness since it illustrates the possibility to design the low-RCS antenna without resorting to a time-consuming full-wave simulations.

V. Conclusion

The use of a suitable hybrid PEC-FSS ground plane for a low-profile microstrip antenna has proved to be an effective means of reducing the radar cross section while preserving the radiation performance of the antenna array. The proposed design does not affect the in-band performance of the radiating device allowing, at the same time, to decrease the out-of-band radar signature of the target. Therefore, it represents the best solution among the investigated ones.

The joint study of the response of the FSS for plane waves and for quasi-TEM waves has revealed a suitable and efficient approach to provide a fast design of a low-RCS antenna, avoiding time-consuming full-wave simulations. Measurements on a real prototype confirm the validity of the proposed design.

Acknowledgment

The authors acknowledge the support of CST for providing additional resources and technical assistance for the parallel version of CST Microwave Studio.

References

[1] J. D. Kraus and R. J. Marhefka, *Antennas*. New York: McGraw-Hill, 2002.
[2] W. Jiang, Y. Liu, S. Gong, and T. Hong, "Application of bionics in antenna radar cross section reduction," *IEEE Antennas Wireless Propag. Lett.*, vol. 8, pp. 1275–1278, 2009.
[3] Y. Li, H. Zhang, Y. Fu, and N. Yuan, "RCS reduction of ridged waveguide slot antenna array using EBG radar absorbing material," *IEEE Antennas Wireless Propag. Lett.*, vol. 7, pp. 473–476, 2008.
[4] H. K. Jang, J. H. Shin, and C. G. Kim, "Low RCS patch array antenna with electromagnetic bandgap using a conducting polymer," in *Proc. ICEAA*, 2010, pp. 140–143.
[5] D. M. Pozar, "RCS reduction for a microstrip antenna using a normally biased ferrite substrate," *IEEE Microw. Guided Wave Lett.*, vol. 2, no. 5, pp. 196–198, May 1992.
[6] J. L. Volakis, A. Alexanian, and J. M. Lin, "Broadband RCS reduction of rectangular patch by using distributed loading," *Electron. Lett.*, vol. 28, no. 25, pp. 2322–2323, 1992.
[7] M. Gustafsson, "RCS reduction of integrated antenna arrays and radomes with resistive sheets," in *Proc. IEEE Antennas Propag. Symp.*, Jul. 2006, pp. 3479–3482.
[8] E. F. Knott, J. F. Shaeffer, and M. T. Tuley, *Radar Cross Section*. Raleigh, NC: SciTech, 2004.
[9] R. B. Green, "The general theory of antenna scattering," Ph.D. dissertation, The Ohio State University, Columbus, OH, Dec. 1963.
[10] J. A. McEntee, "A technique for measuring the scattering aperture and absorption aperture of an antenna," Tech. Rep., 1957 [Online]. Available: http://handle.dtic.mil/100.2/ADA402379
[11] R. C. Hansen, "Relationship between antennas as scatterers and as radiators," *Proc. IEEE*, vol. 77, no. 5, pp. 659–662, May 1989.
[12] N. Misran, R. Cahill, and V. F. Fusco, "RCS reduction technique for reflectarray antennas," *Electron. Lett.*, vol. 39, pp. 1630–1631, Nov. 2003.

[13] W.-T. Wang, S.-X. Gong, X. Wang, H.-W. Yuan, J. Ling, and T.-T. Wan, "RCS reduction of array antenna by using bandstop FSS reflector," *J. Electromagn. Waves Appl.*, vol. 23, no. 11, pp. 1505–1514, 2009.
[14] T. K. Wu, *Frequency Selective Surface and Grid Array*. New York: Wiley, 1995.
[15] F. Costa, S. Genovesi, and A. Monorchio, "On the bandwidth of high-impedance frequency selective surfaces," *IEEE Antennas Wireless Propag. Lett.*, vol. 8, pp. 1341–1344, 2009.
[16] F. Costa, A. Monorchio, and G. Manara, "Efficient analysis of frequency selective surfaces by a simple equivalent circuit approach," *IEEE Antennas Propag. Mag.*, 2012, to be published.
[17] S. Maci, M. Caiazzo, A. Cucini, and M. Casaletti, "A pole-zero matching method for EBG surfaces composed of a dipole FSS printed on a grounded dielectric slab," *IEEE Trans. Antennas Propag.*, vol. 53, no. 1, pp. 70–81, Jan. 2005.
[18] D. M. Pozar, *Microwave Engineering*. New York: Wiley, 1998.
[19] C.-C. Chang, C. Caloz, and T. Itoh, "Analysis of a compact slot resonator in the ground plane for microstrip structures," in *Proc. APMC*, 2001, vol. 3, pp. 1100–1103.
[20] K. Woonphil and L. Bomson, "Modelling and design of 2D UC-PBG structure using transmission line theory," in *Proc. IEEE Antennas Propag. Symp.*, 2002, vol. 3, pp. 780–783.
[21] D. Ahn, J.-S. Park, C.-S. Kim, J. Kim, Y. Qian, and T. Itoh, "A design of the low-pass filter using the novel microstrip defected ground structure," *IEEE Trans. Microw. Theory Tech.*, vol. 49, no. 1, pp. 86–93, Jan. 2001.
[22] CST, Framingham, MA, "CST Microwave Studio," 2010 [Online]. Available: http://www.cst.com/Content/Products/MWS/Overview.aspx

Simone Genovesi (S'99–M'07) received the Laurea degree in telecommunication engineering and the Ph.D. degree in information engineering from the University of Pisa, Pisa, Italy, in 2003 and 2007, respectively.

Since 2003, he has been collaborating with the Electromagnetic Communication Laboratory, Pennsylvania State University (Penn State), University Park. From 2004 to 2006, he was a Research Associate with the ISTI Institute, National Research Council of Italy (ISTI-CNR), Pisa, Italy. He is currently a Research Associate with the University of Pisa. His research is focused on metamaterials, antenna optimization, and evolutionary algorithms.

Filippo Costa (S'07–M'10) was born in Pisa, Italy, in 1980. He received the M.Sc. degree in telecommunication engineering and the Ph.D. degree in applied electromagnetism in electrical and biomedical engineering, electronics, smart sensors, and nanotechnologies from the University of Pisa, Pisa, Italy, in 2006 and 2010, respectively.

From March to August 2009, he was a Visiting Researcher with the Department of Radio Science and Engineering, Helsinki University of Technology, TKK (now Aalto University), Aalto, Finland. Since January 2010, he has been a Postdoctoral Researcher with the University of Pisa. His research is focused on the analysis and modeling of frequency selective surfaces and artificial impedance surfaces with emphasis to their application in electromagnetic absorbing materials, antennas, radomes, waveguide filters, and techniques for retrieving dielectric permittivity of materials.

Agostino Monorchio (S'89–M'96–SM'04–F'12) received the Laurea degree in electronics engineering and the Ph.D. degree in methods and technologies for environmental monitoring from the University of Pisa, Pisa, Italy, in 1991 and 1994, respectively.

During 1995, he joined the Radio Astronomy Group, Arcetri Astrophysical Observatory, Florence, Italy, as a Postdoctoral Research Fellow in the area of antennas and microwave systems. He has been collaborating with the Electromagnetic Communication Laboratory, Pennsylvania State University (Penn State), University Park, and he is an Affiliate of the Computational Electromagnetics and Antennas Research Laboratory. He has been a Visiting Scientist with the University of Granada, Granada, Spain, and with the Communication University of China, Beijing, China. In 2010, he affiliated with the Pisa Section of INFN, the National Institute of Nuclear Physics. He is currently an Associate Professor with the School of Engineering, University of Pisa, and Adjunct Professor with the Italian Naval Academy, Livorno, Italy. He is also an Adjunct Professor with the Department of Electrical Engineering, Penn State. He is on the Teaching Board of the Ph.D. course in "remote sensing" and on the council of the Ph.D. School of Engineering "Leonardo da Vinci," University of Pisa. He has been a reviewer for many scientific journals, and he has been supervising numerous research projects related to applied electromagnetics, commissioned and supported by national companies and public institutions. He is active in a number of areas including computational electromagnetics, microwave metamaterials, antennas and radio propagation for wireless networks, active antennas, and electromagnetic compatibility.

Dr. Monorchio has served as Associate Editor of the IEEE ANTENNAS AND WIRELESS PROPAGATION LETTERS. He received a Summa Foundation Fellowship and a NATO Senior Fellowship.